

# Critical Fermi surfaces in generic dimensions arising from transverse gauge field interactions

Ipsita Mandal<sup>1, 2</sup>

<sup>1</sup>*Faculty of Science and Technology, University of Stavanger, 4036 Stavanger, Norway*

<sup>2</sup>*Nordita, Roslagstullsbacken 23, SE-106 91 Stockholm, Sweden*

We study critical Fermi surfaces in generic dimensions arising from coupling finite-density fermions with transverse gauge fields, by applying the dimensional regularization scheme developed in *Phys. Rev. B* 92, 035141 (2015). We consider the cases of  $U(1)$  and  $U(1) \times U(1)$  transverse gauge couplings, and extract the nature of the renormalization group (RG) flow fixed points as well as the critical scalings. Our analysis allows us to treat a critical Fermi surface of a generic dimension  $m$  perturbatively in an expansion parameter  $\epsilon = (2 - m) / (m + 1)$ . One of our key results is that although the two-loop corrections do not alter the existence of an RG flow fixed line for certain  $U(1) \times U(1)$  theories, which was identified earlier for  $m = 1$  at one-loop order, the third-order diagrams do. However, this fixed line feature is also obtained for  $m > 1$ , where the answer is one-loop exact due to UV/IR mixing.

## Contents

I. Introduction	1
II. Model involving a $U(1)$ transverse gauge field	2
A. Dimensional Regularization	3
B. RG Flows At One-Loop Order	6
C. Higher-Loop Corrections	6
III. Model involving two $U(1)$ transverse gauge fields	7
A. Dimensional Regularization	7
B. RG Flows At One-Loop Order	9
C. Higher-Loop Corrections	9
IV. Conclusion	10
References	11
A. Computation Of The Feynman Diagrams At One-Loop Order	13
1. One-Loop Boson Self-Energy	13
2. One-Loop Fermion Self-Energy	14
3. One-Loop Vertex Correction	16

## I. Introduction

Metallic states that lie beyond the framework of Landau Fermi liquid theory are often dubbed as non-Fermi liquids. It is a theoretically challenging task to study such systems, and consequently there have been intensive efforts dedicated to building a framework to understand them [1–32]. They are also referred to as critical Fermi surface states, as the breakdown of the Fermi liquid theory is brought about by the interplay between the soft fluctuations of the Fermi surface and some gapless bosonic fluctuations. These bosonic degrees of freedom can be massless scalar bosons,

or the transverse components of gauge fields. A similar situation also arises in semimetals, where instead of a Fermi surface, there is a Fermi node interacting with long-ranged (unscreened) Coulomb potential which gives rise to a non-Fermi liquid behaviour [33–36]. Since the quasiparticles are destroyed, there is no obvious perturbative parameter in which one can carry out a controlled expansion, which would ultimately enable us to extract the universal properties.

In this paper, we consider the case when Fermi surfaces are coupled with emergent gauge fields [7, 10, 17, 19, 20, 37–40]. This belongs to the category when the critical boson carries zero momentum, and the quasiparticles lose coherence across the entire Fermi surface. An example when the critical boson with zero momentum is a scalar, is the Ising-nematic critical point [8, 11, 13, 22, 24–27, 41–54]. There are complementary cases when the critical boson carries a finite momentum. Examples include the critical points involving spin density wave (SDW), charge density wave (CDW) [14–16, 23, 28–30], and the FFLO order parameter [32].

An analytic approach [22, 24, 32, 55] to deal with non-Fermi liquid quantum critical points is through dimensional regularization, in which the co-dimension of the Fermi surface is increased in order to identify an upper critical dimension  $d = d_c$ , and subsequently, to calculate the critical exponents in a systematic expansion involving the parameter  $\epsilon = d_c - d_{\text{phys}}$  (where  $d_{\text{phys}}$  is the actual/physical dimension of the system). This approach is especially useful, as it allows one to deal with critical Fermi surfaces of a generic dimension  $m$  [24, 25], representing a system with physical dimensions  $d = d_{\text{phys}} = m + 1$ .

Another approach implements controlled approximation through dynamical tuning, involving an expansion in the inverse of the number ( $N$ ) of fermion flavours combined with a further expansion  $\varepsilon = z_b - 2$ , where  $z_b$  is the dynamical critical exponent of the boson field [10, 17]. This amounts to modifying the kinetic term of a collective mode ( $\phi(k)$ ) from  $k^2 |\phi(k)|^2$  to  $k^{1+\varepsilon} |\phi(k)|^2$ . A drawback of this

approach is that this modification of the kinetic term leads to nonanalyticities in the momentum space, which are equivalent to nonlocal hopping terms in real space. Hence in this paper, we will employ the former approach of dimensional regularization, which maintains locality in real space.

The earlier works considering generic values of  $d$  and  $m$  involved the Ising-nematic order parameter [24, 25], which represents quantum critical metals near a Pomeranchuk transition, where the critical boson couples to antipodal patches with the same sign of coupling strength [13]. In contrast, a transverse gauge field couples to the two antipodal patches with opposite signs [12]. Here, we will implement the dimensional regularization procedure to determine the low-energy scalings of an  $m$ -dimensional (with  $m \geq 1$ ) Fermi surface coupled with one or more transverse gauge fields. First we will develop the formalism for a single  $U(1)$  gauge field. Then we will extend it to the  $U(1) \times U(1)$  case, which can describe a quantum phase transition between a Fermi liquid metal and an electrical insulator without any Fermi surface (deconfined Mott transition), or that between two metals that having Fermi surfaces with finite but different sizes on either side of the transition (deconfined metal-metal transition) [56].

The paper is organized as follows. In Sec. II, we review the framework for applying dimensional regularization scheme to access the non-Fermi liquid fixed points perturbatively, and apply it to the case of a single transverse gauge field. In Sec. III, we carry out the computations for the scenario of quantum critical transitions involving two different kinds of fermions charged differently under the action of two transverse gauge fields. We conclude with a summary and some outlook in Sec. IV. The details of the one-loop calculations have been provided in Appendix A.

## II. Model involving a $U(1)$ transverse gauge field

We first consider an  $m$ -dimensional Fermi surface, which is coupled to a  $U(1)$  transverse gauge field  $a$  in  $d = (m+1)$  space dimensions. The set-up is identical to Ref. [24]. We review it here for the sake of completeness. As in earlier works [22, 24, 25], we want to characterize the resulting non-Fermi liquids through the scaling properties of the fermionic and bosonic Green's functions. To do so, we focus on one point (say  $K^*$ ) of the Fermi surface at which the fermion Green's function is defined. The low energy effective theory involves fermions which are primarily scattered along the tangential directions of the Fermi surface, mediated by the critical boson. We assume the presence of the inversion symmetry, which implies that the fermions near  $K^*$  are most strongly coupled with fermions near the antipodal point  $-K^*$ , since their tangent spaces coincide. Hence we write down a model including a closed Fermi surface divided into two halves centered at momenta  $K^*$  and  $-K^*$  respectively. The fermionic fields  $\psi_{+,j}$  and  $\psi_{-,j}$  represent the corresponding halves, as shown in Fig. 1(a). In

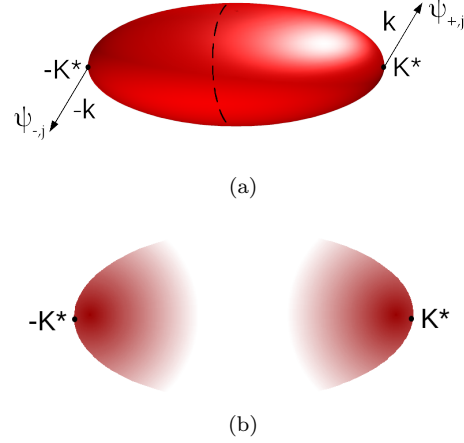


FIG. 1. (a) A compact Fermi surface divided into two halves, centered at  $\pm K^*$ . For each half, a separate fermionic field is introduced. (b) The compact Fermi surface is approximated by two sheets of non-compact Fermi surfaces with a momentum regularization that suppresses modes far away from  $\pm K^*$ .

this coordinate system, the minimal Euclidean action that captures the essential description of the low energy physics is given by [12]:

$$S = \sum_{p=\pm} \sum_{j=1}^N \int dk \psi_{p,j}^\dagger(k) i \left[ k_0 + p k_1 + \mathbf{L}_{(k)}^2 \right] \psi_{p,j}(k) + \frac{1}{2} \int dk \left[ k_0^2 + k_1^2 + \mathbf{L}_{(k)}^2 \right] a^\dagger(k) a(k) + \frac{e}{\sqrt{N}} \sum_{p=\pm} p \sum_{j=1}^N \int dk dq a(q) \psi_{p,j}^\dagger(k+q) \psi_{p,j}(k), \quad (1)$$

where  $k = (k_0, k_1, \mathbf{L}_{(k)})$  is the  $(d+1)$ -dimensional energy-momentum vector with  $dk \equiv \frac{d^{d+1}k}{(2\pi)^{d+1}}$ , and  $e$  is the transverse gauge coupling. The fermion field  $\psi_{+,j}(k_0, k_1)$  ( $\psi_{-,j}(k_0, k_1)$ ) with flavor  $j = 1, 2, \dots, N$ , frequency  $k_0$  and momentum  $K_i^* + k_i$  ( $-K_i^* + k_i$ ) is represented by  $\psi_{+,j}(k_0, k_i)$  ( $\psi_{-,j}(k_0, k_i)$ ), with  $1 \leq i \leq d$ . The components  $k_1$  and  $\mathbf{L}_{(k)} \equiv (k_2, k_3, \dots, k_d)$  represent the momentum components perpendicular and parallel to the Fermi surface at  $\pm K^*$ , respectively. We have rescaled the momentum such that the absolute value of the Fermi velocity and the quadratic curvature of the Fermi surface at  $\pm K^*$  can be set to one. Due to the fact that the Fermi surface is locally parabolic, the scaling dimension of  $k_1$  and  $\mathbf{L}_{(k)}$  are equal to 1 and  $1/2$  respectively. For a generic convex Fermi surface, there can be cubic and higher order terms in  $\mathbf{L}_{(k)}$ , but we can ignore them as they are irrelevant in the renormalization group (RG) sense. Since we have a compact Fermi surface, the range of  $\mathbf{L}_{(k)}$  in  $\int dk$  is finite and is set by the size of the Fermi surface. This range is of the order of  $\sqrt{k_F}$  in this coordinate system. To ensure this finite integration range, we

will include an exponential cut-off  $\exp\left\{-\frac{\mathbf{L}_{(k)}^2}{\mu k_F}\right\}$  while using the fermion Green's function in loop integrations, which will capture the compactness of the Fermi surface in a minimal way without including the details of the shape. This can be made explicit by including the inverse of this factor in the kinetic part of the fermion action.

In order to control the gauge coupling  $e$  for a given  $m$ , we tune the co-dimension of the Fermi surface [22, 23, 55] to determine the upper critical dimension  $d = d_c$ . To preserve the analyticity of the theory in momentum space (locality in real space) with general co-dimensions, we introduce the spinors [22, 23]

$$\Psi_j^T(k) = \left( \psi_{+,j}(k), \psi_{-,j}^\dagger(-k) \right) \text{ and } \bar{\Psi}_j \equiv \Psi_j^\dagger \gamma_0, \quad (2)$$

and write an action that describes the  $m$ -dimensional Fermi surface embedded in a  $d$ -dimensional momentum space:

$$\begin{aligned} S = & \sum_j \int dk \bar{\Psi}_j(k) i[\Gamma \cdot \mathbf{K} + \gamma_{d-m} \delta_k] \Psi_j(k) \exp\left\{\frac{\mathbf{L}_{(k)}^2}{\mu \tilde{k}_F}\right\} \\ & + \frac{1}{2} \int dk \mathbf{L}_{(k)}^2 a^\dagger(k) a(k) \\ & + \frac{e \mu^{x/2}}{\sqrt{N}} \sum_j \int dk dq a(q) \bar{\Psi}_j(k+q) \gamma_0 \Psi_j(k), \\ x = & \frac{4+m-2d}{2}. \end{aligned} \quad (3)$$

Here,  $\mathbf{K} \equiv (k_0, k_1, \dots, k_{d-m-1})$  includes the frequency and the first  $(d-m-1)$  components of the  $d$ -dimensional momentum vector,  $\mathbf{L}_{(k)} \equiv (k_{d-m+1}, \dots, k_d)$  and  $\delta_k = k_{d-m} + \mathbf{L}_{(k)}^2$ . In the  $d$ -dimensional momentum space,  $k_1, \dots, k_{d-m}$  ( $\mathbf{L}_{(k)}$ ) represent(s) the  $(d-m)$  ( $m$ ) directions perpendicular (tangential) to the Fermi surface.  $\Gamma \equiv (\gamma_0, \gamma_1, \dots, \gamma_{d-m-1})$  represents the gamma matrices associated with  $\mathbf{K}$ . Since we are interested in a value of co-dimension  $1 \leq d-m \leq 2$ , we consider only  $2 \times 2$  gamma matrices with  $\gamma_0 = \sigma_y$ ,  $\gamma_{d-m} = \sigma_x$ . In the quadratic action of the boson, only  $\mathbf{L}_{(k)}^2 a^\dagger(k) a(k)$  is kept, because  $|\mathbf{K}|^2 + k_{d-m}^2$  is irrelevant under the scaling where  $k_0, k_1, \dots, k_{d-m}$  have dimension 1 and  $k_{d-m+1}, \dots, k_d$  have dimension 1/2. In the presence of the  $(m+1)$ -dimensional rotational symmetry, all components of  $k_{d-m}, \dots, k_d$  should be equivalent. The rotational symmetry of the bare fermion kinetic part in the  $(d-m)$ -dimensional space spanned by  $\mathbf{K}$  components is destroyed by the coupling with the gauge boson, as the latter involves the  $\gamma_0$  matrix. With this in mind, we will denote the extra (unphysical) co-dimensions by the vector  $\tilde{\mathbf{K}}$ , and the corresponding gamma matrices by  $\tilde{\Gamma}$ .

Since the scaling dimension of the gauge coupling is equal to  $x$ , we have made  $e$  dimensionless by using a mass scale  $\mu$ . We have also defined a dimensionless parameter for the Fermi momentum,  $\tilde{k}_F = k_F/\mu$  using this mass scale. The spinor  $\Psi_j$  exhibits an energy dispersion with

two bands  $E_k = \pm \sqrt{\sum_{i=1}^{d-m-1} k_i^2 + \delta_k^2}$ , and this gives an  $m$ -dimensional Fermi surface embedded in the  $d$ -dimensional momentum space, defined by the  $d-m$  equations:  $k_i = 0$  for  $i = \{1, \dots, d-m-1\}$  and  $k_{d-m} = -\mathbf{L}_{(k)}^2$ . Basically, the extra  $(d-m-1)$  directions are gapped out so that the Fermi surface reduces to a sphere  $S^m$  (sphere in an  $(m+1)$ -dimensional Euclidean space) locally.

When we perform dimensional regularization, the theory implicitly has an ultraviolet (UV) cut-off for  $\mathbf{K}$  and  $k_{d-m}$ , which we denote by  $\Lambda$ . It is natural to choose  $\Lambda = \mu$ , and the theory has two important dimensionless parameters:  $e$  and  $\tilde{k}_F = k_F/\Lambda$ . If  $k$  is the typical energy at which we probe the system, the limit of interest is  $k \ll \Lambda \ll k_F$ . This is because  $\Lambda$  sets the largest energy (equivalently, momentum perpendicular to the Fermi surface) fermions can have, whereas  $k_F$  sets the size of the Fermi surface. We will consider the RG flow generated by changing  $\Lambda$  and requiring that low-energy observables are independent of it. This is equivalent to a coarse-graining procedure of integrating out high-energy modes away from Fermi surface. Because the zero energy modes are not integrated out,  $k_F/\Lambda$  keeps on increasing in the coarse-graining procedure. We treat  $k_F$  as a dimensionful coupling constant that flows to infinity in the low-energy limit. Physically, this describes the fact that the size of the Fermi surface, measured in the unit of the thickness of the thin shell, around the Fermi surface diverges in the low-energy limit. This is illustrated in Fig. 1(a).

### A. Dimensional Regularization

To gain a controlled approximation of the physics of the critical Fermi surface, we fix  $m$  and tune  $d$  towards a critical dimension  $d_c$ , at which quantum corrections depend logarithmically on  $\Lambda$  within the range  $\Lambda \ll k_F$ . In order to identify the value of  $d_c$  as a function of  $m$ , we consider the one-loop quantum corrections.

The bare propagator for fermions is given by:

$$G_0(k) = -i \frac{\Gamma \cdot \mathbf{K} + \gamma_{d-m} \delta_k}{\mathbf{K}^2 + \delta_k^2} \times \exp\left\{-\frac{\mathbf{L}_{(k)}^2}{\mu \tilde{k}_F}\right\}. \quad (4)$$

Since the bare boson propagator is independent of  $k_0, \dots, k_{d-m}$ , the loop integrations involving it are ill-defined, unless one resums a series of diagrams that provides a non-trivial dispersion along those directions. This amounts to rearranging the perturbative expansion such that the one-loop boson self-energy is included at the ‘zero’-th order. The dressed boson propagator, which includes the one-loop

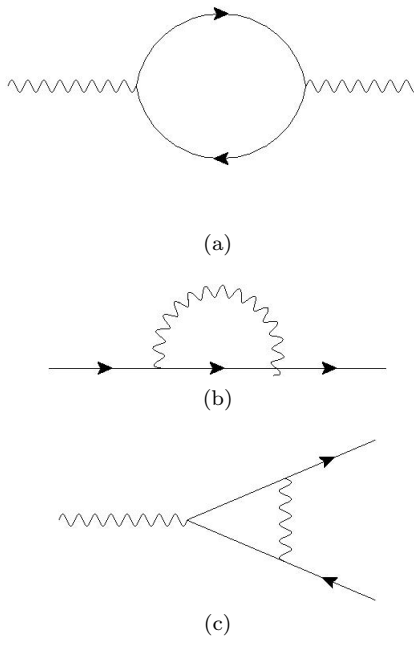


FIG. 2. The one-loop diagrams for (a) the boson self-energy, (b) the fermion self-energy, and (c) the vertex correction. Lines with arrows represent the bare fermion propagator, whereas wiggly lines in (b) and (c) represent the dressed boson propagator which includes the one-loop self-energy in (a).

self-energy (see Fig. 2(a)), is given by:

$$\begin{aligned} \Pi_1(k) &= -e^2 \mu^x \int dq \text{Tr} [\gamma_0 G_0(k+q) \gamma_0 G_0(q)] \\ &= -\frac{\beta(d, m) e^2 \mu^x (\mu \tilde{k}_F)^{\frac{m-1}{2}}}{|\mathbf{L}_{(q)}|} \\ &\times [k_0^2 + (m+1-d) \tilde{\mathbf{K}}^2] |\mathbf{K}|^{d-m-2}, \end{aligned} \quad (5)$$

where

$$\beta(d, m) = \frac{\pi^{\frac{4-d}{2}} \Gamma(d-m) \Gamma(m+1-d)}{2^{\frac{4d-m-1}{2}} \Gamma^2(\frac{d-m+2}{2}) \Gamma(\frac{m+1-d}{2})}. \quad (6)$$

This expression is valid to the leading order in  $k/k_F$ , and for  $|\mathbf{K}|^2/|\mathbf{L}_{(k)}|^2, \delta_k^2/|\mathbf{L}_{(k)}|^2 \ll k_F$  [57]. We provide the details of computation for the expression of  $\Pi_1(k)$  in Appendix A 1. For  $m > 1$ , the boson self-energy diverges in

the  $k_F \rightarrow \infty$  limit. This is due to the fact that the Landau damping gets stronger for a system with a larger Fermi surface, as the boson can decay into particle-hole excitations that encompass the entire Fermi surface for  $m > 1$ . This is in contrast with the case for  $m = 1$ , where a low-energy boson with a given momentum can decay into particle-hole excitations only near the isolated patches whose tangent vectors are parallel to that momentum. Eq. (5) is valid when there exists at least one direction that is tangential to the Fermi surface ( $m \geq 1$ ). Henceforth, we will use the dressed propagator:

$$D_1(q) = \frac{1}{\mathbf{L}_{(q)}^2 - \Pi_1(q)}. \quad (7)$$

for any loop calculation.

The next step is to compute the one-loop fermion self-energy  $\Sigma_1(q)$ , as shown in Fig. 2(b). Again, the details of the calculation are provided in Appendix A 2. This blows up logarithmically in  $\Lambda$  at the critical dimension

$$d_c(m) = m + \frac{3}{m+1}. \quad (8)$$

The physical dimension is given by  $d = d_c(m) - \epsilon$ . In the dimensional regularization scheme, the logarithmic divergence in  $\Lambda$  turns into a pole in  $\frac{1}{\epsilon}$ :

$$\begin{aligned} \Sigma_1(q) &= -\frac{i e^{\frac{2(m+1)}{3}} [u_0 \gamma_0 q_0 + u_1 (\tilde{\mathbf{F}} \cdot \tilde{\mathbf{Q}})]}{N \tilde{k}_F^{\frac{(m-1)(2-m)}{6}} \epsilon} \\ &+ \text{finite terms} \end{aligned} \quad (9)$$

to the leading order in  $q/k_F$ , where  $u_0, u_1 \geq 0$ . For the cases of interest, we have computed these coefficients numerically to obtain:

$$\begin{cases} u_0 = 0.0201044, & v_0 = 1.85988 \quad \text{for } m = 1 \\ u_0 = v_0 = 0.0229392 & \quad \text{for } m = 2 \end{cases}. \quad (10)$$

The one-loop vertex correction in Fig. 2(c) is non-divergent, and hence does not contribute to the RG flows. This is to be contrasted with the Ising-nematic case where it is guaranteed to vanish due to a Ward identity [22].

We can vary the dimension of Fermi surface from  $m = 1$  to  $m = 2$  while keeping  $\epsilon$  small, thus providing a controlled description for any  $m$  between 1 and 2. For a given  $m$ , we tune  $d$  such that  $\epsilon = d_c(m) - d$  is small. To remove the UV divergences in the  $\epsilon \rightarrow 0$  limit, we add counterterms using the minimal subtraction scheme. The counter terms take the same form as the original local action:

$$\begin{aligned}
S_{CT} = & \sum_j \int dk \bar{\Psi}_j(k) i \left[ A_0 \gamma_0 k_0 + A_1 \tilde{\Gamma} \cdot \tilde{\mathbf{K}} + A_2 \gamma_{d-m} \delta_k \right] \Psi_j(k) \exp \left\{ \frac{\mathbf{L}_{(k)}^2}{\mu \tilde{k}_F} \right\} \\
& + \frac{A_3}{2} \int dk \mathbf{L}_{(k)}^2 a^\dagger(k) a(k) + A_4 \frac{i e \mu^{x/2}}{\sqrt{N}} \sum_j \int dk dq a(q) \bar{\Psi}_j(k+q) \gamma_0 \Psi_j(k),
\end{aligned} \tag{11}$$

where

$$A_\zeta = \sum_{\lambda=1}^{\infty} \frac{Z_\zeta^{(\lambda)}(e, \tilde{k}_F)}{\epsilon^\lambda} \text{ with } \zeta = 0, 1, 2, 3, 4. \tag{12}$$

In the mass-independent minimal subtraction scheme, these coefficients depend only on the scaled coupling  $e$ , and the scaled Fermi momentum  $\tilde{k}_F$ . As discussed earlier, we expect  $\tilde{k}_F$  to act as another coupling for  $m > 1$ , and hence it must be included in the RG flow equations. The coefficients can be further expanded in the number of loops modulo the one-loop self-energy of boson, which is already included in Eq. (7). Note that the  $(d-m-1)$ -dimensional rotational invariance in the space perpendicular to the Fermi surface guarantees that each term in  $\tilde{\Gamma} \cdot \tilde{\mathbf{K}}$  is renormalized in the

same way. Similarly, the sliding symmetry along the Fermi surface guarantees that the form of  $\delta_k$  is preserved. However,  $A_0$ ,  $A_1$  and  $A_2$  are in general different due to a lack of the full rotational symmetry in the  $(d+1)$ -dimensional spacetime. Note the difference from the Ising-nematic case, where we had  $A_0 = A_1$ , as the rotational symmetry there involved the full  $(d-m)$ -dimensional subspace.

Adding the counterterms to the original action, we obtain the renormalized action which gives the finite quantum effective action:

$$\begin{aligned}
S_{ren} = & \sum_j \int dk^B \bar{\Psi}_j^B(k^B) i \left[ \mathbf{\Gamma} \cdot \mathbf{K}^B + \gamma_{d-m} \delta_{k^B} \right] \Psi_j^B(k^B) \exp \left\{ \frac{\mathbf{L}_{(k^B)}^2}{k_{FB}} \right\} + \frac{1}{2} \int dk^B \mathbf{L}_{(k^B)}^2 a^{B\dagger}(k^B) a^B(k^B) \\
& + \frac{i e^B}{\sqrt{N}} \sum_j \int dk^B dq^B a^B(q^B) \bar{\Psi}_j^B(k^B + q^B) \gamma_0 \Psi_j^B(k^B),
\end{aligned} \tag{13}$$

where

$$\begin{aligned}
k_0^B &= \frac{Z_0}{Z_2} k_0, \quad \tilde{\mathbf{K}}^B = \frac{Z_1}{Z_2} \tilde{\mathbf{K}}, \quad k_{d-m}^B = k_{d-m}, \\
\mathbf{L}_{(k^B)} &= \mathbf{L}_{(k)}, \quad \Psi_j^B(k^B) = Z_\Psi^{\frac{1}{2}} \Psi_j(k), \\
a^B(k^B) &= Z_a^{\frac{1}{2}} a(k), \quad k_F^B = k_F = \mu \tilde{k}_F, \\
Z_\Psi &= \frac{Z_2^{d-m+1}}{Z_0 Z_1^{d-m-1}}, \quad Z_a = \frac{Z_3 Z_2^{d-m}}{Z_0 Z_1^{d-m-1}}, \\
e^B &= Z_e e \mu^{\frac{x}{2}}, \quad Z_e = \frac{Z_4 Z_2^{\frac{d-m-1}{2}}}{\sqrt{Z_0 Z_3} Z_1^{\frac{d-m-1}{2}}}.
\end{aligned} \tag{14}$$

Here,

$$Z_\zeta = 1 + A_\zeta. \tag{15}$$

The superscript ‘‘B’’ denotes the bare fields, couplings, and momenta. In Eq. (13), there is a freedom to change the

renormalizations of the fields and the renormalization of momentum without affecting the action. Here we fix the freedom by requiring that  $\delta_{k^B} = \delta_k$ . This amounts to measuring scaling dimensions of all other quantities relative to that of  $\delta_k$ .

Let  $z$  be the dynamical critical exponent,  $\tilde{z}$  be the critical exponent along the extra spatial dimensions,  $\beta_e$  be the beta function for the coupling  $e$ ,  $\beta_{k_F}$  be the beta function for  $\tilde{k}_F$ , and  $\eta_\Psi$  ( $\eta_\phi$ ) be the anomalous dimension for the fermions (gauge boson). These are explicitly given by:

$$\begin{aligned}
z &= 1 + \frac{\partial \ln(Z_0)}{\partial \ln \mu}, \quad \tilde{z} = 1 + \frac{\partial \ln(Z_1)}{\partial \ln \mu}, \quad \eta_\Psi = \frac{1}{2} \frac{\partial \ln Z_\Psi}{\partial \ln \mu}, \\
\eta_a &= \frac{1}{2} \frac{\partial \ln Z_a}{\partial \ln \mu}, \quad \beta_{k_F}(\tilde{k}_F) = \frac{\partial \tilde{k}_F}{\partial \ln \mu}, \quad \beta_e = \frac{\partial e}{\partial \ln \mu}.
\end{aligned} \tag{16}$$

In the  $\epsilon \rightarrow 0$  limit, we require solutions of the form:

$$\begin{aligned} z &= z^{(0)}, \quad \tilde{z} = \tilde{z}^{(0)}, \\ \eta_\Psi &= \eta_\Psi^{(0)} + \eta_\Psi^{(1)}\epsilon, \quad \eta_a = \eta_a^{(0)} + \eta_a^{(1)}\epsilon. \end{aligned} \quad (17)$$

## B. RG Flows At One-Loop Order

To one-loop order, the counterterms are given by  $Z_\zeta = 1 + \frac{Z_\zeta^{(1)}}{\epsilon}$ . Collecting all the results, we find that only

$$Z_0^{(1)} = -\frac{u_0 \tilde{e}}{N} \text{ and } Z_1^{(1)} = -\frac{u_1 \tilde{e}}{N} \quad (18)$$

are nonzero, where

$$\tilde{e} = \frac{e^{\frac{2(m+1)}{3}}}{\tilde{k}_F^{\frac{(m-1)(2-m)}{6}}}. \quad (19)$$

Then the one-loop beta functions, that dictate the flow of  $\tilde{k}_F$  and  $e$  with the increasing energy scale  $\mu$ , are given by:

$$\begin{aligned} \beta_{k_F} &= -\tilde{k}_F, \quad (1-z)Z_0 = -\beta_e \frac{\partial Z_0}{\partial e} + \tilde{k}_F \frac{\partial Z_0}{\partial \tilde{k}_F}, \\ (1-\tilde{z})Z_1 &= -\beta_e \frac{\partial Z_1}{\partial e} + \tilde{k}_F \frac{\partial Z_1}{\partial \tilde{k}_F}, \\ \beta_e &= -\frac{\epsilon + \frac{2-m}{m+1}(1-\tilde{z}) + 1-z}{2} e, \\ \eta_\Psi &= \eta_a = \frac{1-z+(1-\tilde{z})(d-m-1)}{2}. \end{aligned} \quad (20)$$

Solving these equations using the required form outlined in Eq. (17), we get:

$$\begin{aligned} z &= 1 - \frac{(m+1)u_0 \tilde{e}}{3N + (m+1)u_1 \tilde{e}}, \\ \tilde{z} &= 1 - \frac{(m+1)u_1 \tilde{e}}{3N + (m+1)u_1 \tilde{e}}, \\ -\frac{\beta_e}{e} &= \frac{\epsilon}{2} + \frac{(m-1)(2-m)}{4(m+1)} - \frac{(m+1)u_0 + (2-m)u_1}{6N} \tilde{e}. \end{aligned} \quad (21)$$

The first term indicates that  $e$  remains strictly relevant in the infrared (IR) at  $d = d_c(m)$  for  $1 < m < 2$ . However, the second term implies that the higher order corrections are controlled not by  $e$ , but by an effective coupling  $\tilde{e}$ . Indeed, the scaling dimension of  $\tilde{e}$  vanishes at  $d_c$  for  $1 \leq m \leq 2$ . The beta function of this effective coupling is given by:

$$\frac{\beta_{\tilde{e}}}{\tilde{e}} = -\frac{(m+1)\epsilon}{3} + \frac{(m+1)[(m+1)u_0 + (2-m)u_1]}{9N} \tilde{e}. \quad (22)$$

The interacting fixed point is obtained from  $\beta_{\tilde{e}} = 0$ , and takes the form:

$$\tilde{e}^* = \frac{3N\epsilon}{(m+1)u_0 + (2-m)u_1} + \mathcal{O}(\epsilon^2). \quad (23)$$

It can be checked that this is an IR stable fixed point by computing the first derivative of  $\beta_{\tilde{e}}$ . The critical exponents at this stable fixed point are given by:

$$\begin{aligned} z^* &= 1 + \frac{(m+1)u_1\epsilon}{(m+1)u_0 + (2-m)u_1}, \\ \tilde{z}^* &= 1 + \frac{(m+1)u_0\epsilon}{(m+1)u_0 + (2-m)u_1}, \\ \eta_\Psi^* &= \eta_a^* = -\frac{\epsilon}{2}. \end{aligned} \quad (24)$$

## C. Higher-Loop Corrections

We will now discuss the implications of the higher-loop corrections, without actually computing the Feynman diagrams. For  $m > 2$ , we expect a nontrivial UV/IR mixing to be present, as was found in Ref. 24 and 25, which makes the results one-loop exact. In other words, all higher-loop corrections would vanish for  $m > 1$  in the limit  $k_F \rightarrow 0$ , due to suppression of the results by positive powers of  $k_F$ . For  $m = 1$ , we will use the arguments and results of Ref. 22 to assume a generic form of the corrections coming from two-loop diagrams. Henceforth, we will just focus on  $m = 1$  in this subsection.

The two-loop bosonic self-energy should turn out to be UV finite, and hence will renormalize the factor  $\beta(\frac{5}{2}, 1)$  (see Eq. 6) by a finite amount  $\beta_2 = \frac{\kappa \tilde{e}}{N}$ , where  $\kappa$  is a finite number. Then the bosonic propagator at this order will take the form:

$$D_2(q) = \frac{1}{\mathbf{L}_{(q)}^2 + \frac{[\beta(\frac{5}{2}, 2) + \frac{\kappa \tilde{e}}{N}]e^2\mu^\epsilon}{|\mathbf{L}_{(q)}|} \times \frac{\kappa_0^2 + (\epsilon - \frac{1}{2})\mathbf{K}^2}{|\mathbf{K}|^{\frac{1}{2} + \epsilon}}}. \quad (25)$$

From this, the fermion self-energy now receives a correction

$$\begin{aligned} \Sigma_2^{(1)}(k) &= \left[ \left\{ \frac{\beta(\frac{5}{2}, 2)}{\beta(\frac{5}{2}, 2) + \frac{\kappa \tilde{e}}{N}} \right\}^{\frac{1}{3}} - 1 \right] \Sigma_1(k) \\ &= -\frac{\kappa \tilde{e}}{3N\beta(\frac{5}{2}, 2)} \Sigma_1(k) + \text{finite terms}. \end{aligned} \quad (26)$$

Now the two-loop fermion self-energy diagrams, after taking into account the counterterms obtained from one-loop corrections, take the form:

$$\begin{aligned} \Sigma_2^{(2)}(k) &= -\frac{i\tilde{e}^2 \left[ \tilde{v}_0 \gamma_0 q_0 + \tilde{v}_1 (\tilde{\Gamma} \cdot \tilde{\mathbf{Q}}) + w \gamma_{d-1} \delta_k \right]}{N^2 \epsilon} \\ &+ \text{finite terms}. \end{aligned} \quad (27)$$

Adding the two, generically the total two-loop fermion self-energy can be written as:

$$\Sigma_2^{(2)}(k) = -\frac{i\tilde{e}^2 \left[ v_0 \gamma_0 q_0 + v_1 \left( \tilde{\Gamma} \cdot \tilde{\mathbf{Q}} \right) + w \gamma_{d-1} \delta_k \right]}{N^2 \epsilon} + \text{finite terms.} \quad (28)$$

There will also be a divergent vertex correction which will

lead to a nonzero  $Z_4^{(1)}$  of the form  $-\frac{\tilde{e}^2 \mu^{\frac{4\epsilon}{3}} y}{N^2}$ . All these now lead to the nonzero coefficients:

$$\begin{aligned} Z_0^{(1)} &= -\frac{u_0 \tilde{e}}{N} - \frac{v_0 \tilde{e}^2}{N^2}, & Z_1^{(1)} &= -\frac{u_1 \tilde{e}}{N} - \frac{v_0 \tilde{e}^2}{N^2}, \\ Z_2^{(1)} &= -\frac{w \tilde{e}^2}{N^2}, & Z_4^{(1)} &= -\frac{y \tilde{e}^2}{N^2}, \end{aligned} \quad (29)$$

resulting in

$$\frac{\beta_{\tilde{e}}}{\tilde{e}} = -\frac{2 \{2 u_1 \tilde{e} + 3 N\} \epsilon}{9 N} + \frac{2 \{2 \tilde{e} (2 u_0 u_1 + u_1^2 + 6 v_0 + 3 v_1 - 9 w) + 3 N (2 u_0 + u_1)\} \tilde{e}}{27 N^2}. \quad (30)$$

At the fixed point, we now have:

$$\frac{\tilde{e}^*}{N} = \frac{3 \epsilon}{2 u_0 + u_1} - \frac{18 (2 v_0 + v_1 - 3 w)}{(2 u_0 + u_1)^3} \epsilon^2 + \mathcal{O}(\epsilon^3). \quad (31)$$

This shows that the nature of the stable non-Fermi liquid fixed point remains unchanged, although its location (as well as any critical scaling) gets corrected by one higher power of  $\epsilon$ .

### III. Model involving two $U(1)$ transverse gauge fields

In this section, we consider the  $m$ -dimensional Fermi surfaces of two different kinds of fermions (denoted by subscripts 1 and 2) coupled to two  $U(1)$  gauge fields,  $a_c$  and  $a_s$ , in the context of deconfined Mott transition and deconfined metal-metal transition studied in Ref. 56 (for  $m = 1$ ). The fermion fields  $\psi_{1,\pm,j}$  and  $\psi_{2,\pm,j}$  carry negative charges under the even ( $a_c + a_s$ ) and odd ( $a_c - a_s$ ) combinations of the gauge fields, and hence the action takes the form:

$$\begin{aligned} S = & \sum_{\alpha=1,2} \sum_{p=\pm} \sum_{j=1}^N \int dk \psi_{\alpha,p,j}^\dagger(k) \left[ i k_0 + p k_{d-m} + \mathbf{L}_{(k)}^2 \right] \psi_{\alpha,p,j}(k) + \frac{1}{2} \int dk \mathbf{L}_{(k)}^2 [a_c^\dagger(k) a_c(k) + a_s^\dagger(k) a_s(k)] \\ & + \sum_{\alpha=1,2} \sum_{p=\pm} p \sum_{j=1}^N \int dk dq \left[ \frac{(-1)^\alpha e_s}{\sqrt{N}} a_s(q) \psi_{\alpha,p,j}^\dagger(k+q) \psi_{\alpha,p,j}(k) - \frac{e_c}{\sqrt{N}} a_c(q) \psi_{\alpha,p,j}^\dagger(k+q) \psi_{\alpha,p,j}(k) \right], \end{aligned} \quad (32)$$

where  $e_c$  and  $e_s$  denote the gauge couplings for the gauge fields  $a_c$  and  $a_s$  respectively. We will perform dimensional regularization on this action and determine the RG fixed points. Our formalism allows us to extend the discussion beyond  $m = 1$ , and also to easily compute higher-loop corrections.

#### A. Dimensional Regularization

Proceeding as in the single transverse gauge field case, we add artificial co-dimensions for dimensional regularization after introducing the two-component spinors:

$$\Psi_{\alpha,j}^T(k) = \left( \psi_{\alpha,+j}(k), \psi_{\alpha,-j}^\dagger(-k) \right) \text{ and } \bar{\Psi}_{\alpha,j} \equiv \Psi_{\alpha,j}^\dagger \gamma_0, \quad (33)$$

with  $\alpha = 1, 2$ .

The dressed gauge boson propagators, including the one-loop self-energies, are given by:

$$\begin{aligned} \Pi_1^c(k) = & -\frac{\beta(d, m) e_c^2 \mu^x \left( \mu \tilde{k}_F \right)^{\frac{m-1}{2}}}{|\mathbf{L}_{(q)}|} \\ & \times \left[ k_0^2 + (m+1-d) \tilde{\mathbf{K}}^2 \right] |\mathbf{K}|^{d-m-2}, \end{aligned} \quad (34)$$

and

$$\begin{aligned} \Pi_1^s(k) = & -\frac{\beta(d, m) e_s^2 \mu^x \left( \mu \tilde{k}_F \right)^{\frac{m-1}{2}}}{|\mathbf{L}_{(q)}|} \\ & \times \left[ k_0^2 + (m+1-d) \tilde{\mathbf{K}}^2 \right] |\mathbf{K}|^{d-m-2}, \end{aligned} \quad (35)$$

for the  $a_c$  and  $a_s$  gauge fields, respectively. This implies that the one-loop fermion self-energy for both  $\Psi_{1,j}$  and  $\Psi_{2,j}$

now takes the form:

$$\Sigma_1(q) = -\frac{i \left( e_c^{\frac{2(m+1)}{3}} + e_s^{\frac{2(m+1)}{3}} \right) u_0 \gamma_0 q_0 + u_1 (\tilde{\Gamma} \cdot \tilde{\mathbf{Q}})}{N \tilde{k}_F^{\frac{(m-1)(2-m)}{6}} \epsilon} + \text{finite terms}, \quad (36)$$

with the critical dimension  $d_c = \left(m + \frac{3}{m+1}\right)$ ,  $u_0$  and  $u_1$  (See Eq. 10) having the same values as for the  $U(1)$  case.

The counterterms take the same form as the original local action:

---


$$S_{CT} = \sum_{\alpha,j} \int dk \bar{\Psi}_{\alpha,j}(k) i \left[ A_0 \gamma_0 k_0 + A_1 \tilde{\Gamma} \cdot \tilde{\mathbf{K}} + A_2 \gamma_{d-m} \delta_k \right] \Psi_{\alpha,j}(k) \exp \left\{ \frac{\mathbf{L}_{(k)}^2}{\mu \tilde{k}_F} \right\} + \frac{A_{3s}}{2} \int dk \mathbf{L}_{(k)}^2 a_s^\dagger(k) a_s(k) \\ + \frac{A_{3c}}{2} \int dk \mathbf{L}_{(k)}^2 a_c^\dagger(k) a_c(k) - A_{4c} \frac{e_c \mu^{x/2}}{\sqrt{N}} \sum_{\alpha,j} \int dk dq a_c(q) \bar{\Psi}_{\alpha,j}(k+q) \gamma_0 \Psi_{\alpha,j}(k) \\ + A_{4s} \frac{e_s \mu^{x/2}}{\sqrt{N}} \sum_{\alpha,j} (-1)^\alpha \int \frac{d^{d+1}k d^{d+1}q}{(2\pi)^{2d+2}} a_s(q) \bar{\Psi}_{\alpha,j}(k+q) \gamma_0 \Psi_{\alpha,j}(k), \quad (37)$$

where

$$A_\zeta = \sum_{\lambda=1}^{\infty} \frac{Z_\zeta^{(\lambda)}(e, \tilde{k}_F)}{\epsilon^\lambda} \text{ with } \zeta = 0, 1, 2, 3_c, 3_s, 4_c, 4_s. \quad (38)$$


---

We have taken into account the exchange symmetry:  $\Psi_{1,j} \leftrightarrow \Psi_{2,j}$ ,  $a_s \rightarrow -a_s$ , which was assumed in Ref. 56, and here it means that both  $\Psi_{1,j}$  and  $\Psi_{2,j}$  have the same

wavefunction renormalization  $Z_\Psi^{1/2}$ .

Adding the counterterms to the original action, we obtain the renormalized action:

---


$$S_{ren} = \sum_{\alpha,j} \int dk^B \bar{\Psi}_{\alpha,j}^B(k^B) i \left[ \gamma_0 k_0^B + \tilde{\Gamma} \cdot \tilde{\mathbf{K}}^B + \gamma_{d-m} \delta_k \right] \Psi_{\alpha,j}^B(k^B) \exp \left\{ \frac{\mathbf{L}_{(k^B)}^2}{\mu \tilde{k}_F^B} \right\} + \frac{1}{2} \int dk^B \mathbf{L}_{(k^B)}^2 a_c^{B\dagger}(k^B) a_c^B(k^B) \\ + \frac{1}{2} \int dk^B \mathbf{L}_{(k^B)}^2 a_s^{B\dagger}(k^B) a_s^B(k^B) - \frac{e_c^B \mu^{x/2}}{\sqrt{N}} \sum_{\alpha,j} \int dk^B dq^B a_c^B(q^B) \bar{\Psi}_{\alpha,j}^B(k^B + q^B) \gamma_0 \Psi_{\alpha,j}^B(k^B) \\ + \frac{e_s^B \mu^{x/2}}{\sqrt{N}} \sum_{\alpha,j} (-1)^\alpha \int dk^B dq^B a_s^B(q^B) \bar{\Psi}_{\alpha,j}^B(k^B + q^B) \gamma_0 \Psi_{\alpha,j}^B(k^B), \quad (39)$$

remembering that  $\delta_{k^B} = \delta_k$ . Here

$$k_0^B = \frac{Z_0}{Z_2} k_0, \quad \tilde{\mathbf{K}}^B = \frac{Z_1}{Z_2} \tilde{\mathbf{K}}, \quad k_{d-m}^B = k_{d-m}, \quad \mathbf{L}_{(k^B)} = \mathbf{L}_{(k)}, \quad k_F^B = k_F = \mu \tilde{k}_F, \quad \Psi_j^B(k^B) = Z_\Psi^{\frac{1}{2}} \Psi_j(k), \\ a_c^B(k^B) = Z_{a_c}^{\frac{1}{2}} a_c(k), \quad a_s^B(k^B) = Z_{a_s}^{\frac{1}{2}} a_s(k), \quad Z_\Psi = \frac{Z_2^{d-m+1}}{Z_0 Z_1^{d-m-1}}, \quad Z_{a_c} = \frac{Z_{3s} Z_2^{d-m}}{Z_0 Z_1^{d-m-1}}, \quad Z_{a_s} = \frac{Z_{3c} Z_2^{d-m}}{Z_0 Z_1^{d-m-1}}, \\ e_c^B = Z_{e_c} e_c \mu^{\frac{x}{2}}, \quad Z_{e_c} = \frac{Z_4 Z_2^{\frac{d-m}{2}-1}}{\sqrt{Z_0 Z_{3c}} Z_1^{\frac{d-m-1}{2}}}, \quad e_s^B = Z_{e_s} e_s \mu^{\frac{x}{2}}, \quad Z_{e_s} = \frac{Z_4 Z_2^{\frac{d-m}{2}-1}}{\sqrt{Z_0 Z_{3s}} Z_1^{\frac{d-m-1}{2}}}, \quad (40)$$


---

and

$$Z_\zeta = 1 + A_\zeta. \quad (41)$$

As before, the superscript “B” denotes the bare fields, cou-

plings, and momenta.

As before, we will use the same notations, namely,  $z$  for the dynamical critical exponent,  $\tilde{z}$  be the critical exponent along the extra spatial dimensions,  $\beta_{k_F}$  for the the beta function for  $\tilde{k}_F$ , and  $\eta_\psi$  for the anomalous dimension for fermion. Since we have now two gauge fields now, we will use the symbols  $\beta_{e_c}$  and  $\beta_{e_s}$  to denote the beta functions for the couplings  $e_c$  and  $e_s$  respectively, which are explicitly given by:

$$\beta_{e_c} = \frac{\partial e_c}{\partial \ln \mu}, \quad \beta_{e_s} = \frac{\partial e_s}{\partial \ln \mu}. \quad (42)$$

The anomalous dimensions of these two bosons are indicated by:

$$\eta_{a_c} = \frac{1}{2} \frac{\partial \ln Z_{a_c}}{\partial \ln \mu}, \quad \eta_{a_s} = \frac{1}{2} \frac{\partial \ln Z_{a_s}}{\partial \ln \mu}. \quad (43)$$

## B. RG Flows At One-Loop Order

To one-loop order, the counterterms are given by  $Z_\zeta = 1 + \frac{Z_\zeta^{(1)}}{\epsilon}$ . Here, only

$$Z_0^{(1)} = -\frac{u_0(\tilde{e}_c + \tilde{e}_s)}{N} \text{ and } Z_1^{(1)} = -\frac{u_1(\tilde{e}_c + \tilde{e}_s)}{N} \quad (44)$$

are nonzero, where

$$\tilde{e}_c = \frac{\frac{2(m+1)}{3}}{\tilde{k}_F^{\frac{(m-1)(2-m)}{6}}} \text{ and } \tilde{e}_s = \frac{\frac{2(m+1)}{3}}{\tilde{k}_F^{\frac{(m-1)(2-m)}{6}}}. \quad (45)$$

The one-loop beta functions are now given by:

$$\begin{aligned} \beta_{k_F} &= -\tilde{k}_F, \\ (1-z)Z_0 &= -\beta_{e_c} \frac{\partial Z_0}{\partial e_c} - \beta_{e_s} \frac{\partial Z_0}{\partial e_s} + \tilde{k}_F \frac{\partial Z_0}{\partial \tilde{k}_F}, \\ (1-\tilde{z})Z_1 &= -\beta_{e_c} \frac{\partial Z_1}{\partial e_c} - \beta_{e_s} \frac{\partial Z_1}{\partial e_s} + \tilde{k}_F \frac{\partial Z_1}{\partial \tilde{k}_F}, \\ \beta_{e_c} &= -\frac{\epsilon + \frac{2-m}{m+1}(1-\tilde{z}) + 1-z}{2} e_c, \\ \beta_{e_s} &= -\frac{\epsilon + \frac{2-m}{m+1}(1-\tilde{z}) + 1-z}{2} e_s, \\ \eta_\psi = \eta_{a_c} = \eta_{a_s} &= \frac{1-z+(1-\tilde{z})(d-m-1)}{2}. \end{aligned} \quad (46)$$

Solving these equations, we get:

$$\begin{aligned} -\frac{\beta_{e_c}}{e_c} &= -\frac{\beta_{e_s}}{e_s} \\ &= \frac{\epsilon}{2} + \frac{(m-1)(2-m)}{4(m+1)} - \frac{[(m+1)u_0 + (2-m)u_1](\tilde{e}_c + \tilde{e}_s)}{6N} \end{aligned} \quad (47)$$

Again, it is clear that for generic  $m$ , the order by order loop corrections are controlled not by  $e_c$  and  $e_s$ , but by the effective couplings  $\tilde{e}_c$  and  $\tilde{e}_s$ . Hence we need to compute the RG flows from the beta functions of these effective couplings, which are given by:

$$\begin{aligned} -\frac{\beta_{\tilde{e}_c}}{\tilde{e}_c} &= -\frac{\beta_{\tilde{e}_s}}{\tilde{e}_s} \\ &= \frac{(m+1)\epsilon}{3} - \frac{(m+1)[(m+1)u_0 + (2-m)u_1](\tilde{e}_c + \tilde{e}_s)}{9N} \end{aligned} \quad (48)$$

The interacting fixed points are determined from the zeros of the above beta functions, and take the form:

$$\tilde{e}_c^* + \tilde{e}_s^* = \frac{3N\epsilon}{(m+1)u_0 + (2-m)u_1} + \mathcal{O}(\epsilon^2), \quad (49)$$

which actually give rise to a fixed line, as found in Ref. [56] for the case of  $m = 1$ . It can be checked that this is IR stable by computing the first derivative of the beta functions. Hence, we have proven that the fixed line feature survives for critical Fermi surfaces of dimensions more than one. The critical exponents at this stable fixed line take the same forms as in Eq. (24).

## C. Higher-Loop Corrections

Using the same arguments as the single gauge field case, we will have the following nonzero  $Z_\zeta^{(1)}$ 's:

$$\begin{aligned} Z_0^{(1)} &= -\frac{u_0(\tilde{e}_c + \tilde{e}_s)}{N\epsilon} - \frac{v_0(\tilde{e}_s + \tilde{e}_c)^2}{N^2\epsilon}, \\ Z_1^{(1)} &= -\frac{u_1(\tilde{e}_s + \tilde{e}_c)}{N\epsilon} - \frac{v_1(\tilde{e}_s + \tilde{e}_c)^2}{N^2\epsilon}, \quad Z_2^{(1)} = -\frac{w(\tilde{e}_c + \tilde{e}_s)^2}{N^2\epsilon}, \\ Z_{4_s}^{(1)} &= -\frac{y_s(\tilde{e}_c + \tilde{e}_s)^2}{N^2\epsilon}, \quad Z_{4_c}^{(1)} = -\frac{y_c(\tilde{e}_c + \tilde{e}_s)^2}{N^2\epsilon}, \end{aligned} \quad (50)$$

including the one-loop and two-loop corrections for  $m = 1$ . This leads to the beta functions:

$$\frac{\beta_{\tilde{e}_c}}{\tilde{e}_c} = \frac{\beta_{\tilde{e}_s}}{\tilde{e}_s} = -\frac{2\{2u_1(\tilde{e}_c + \tilde{e}_s) + 3N\}\epsilon}{9N} + \frac{2\{2(\tilde{e}_c + \tilde{e}_s)(2u_0u_1 + u_1^2 + 6v_0 + 3v_1 - 9w) + 3N(2u_0 + u_1)\}(\tilde{e}_c + \tilde{e}_s)}{27N^2}, \quad (51)$$

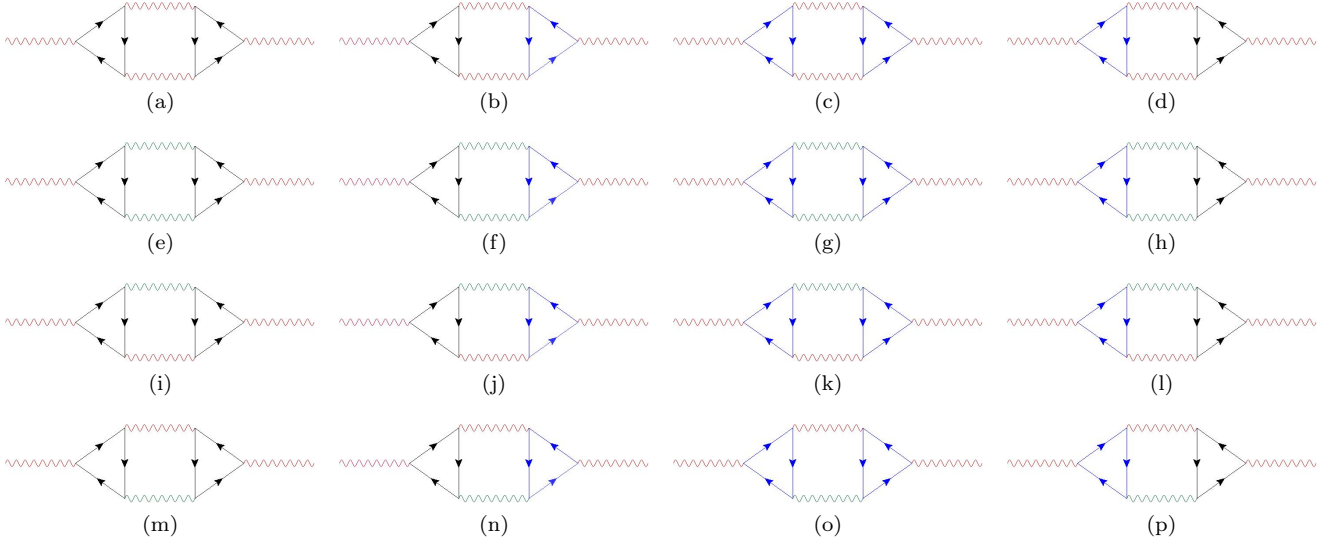


FIG. 3. Contributions from the Aslamazov-Larkin diagrams in the particle-particle channels to the three-loop boson self-energy of the  $a_c$  transverse gauge field. The red and green wavy lines denote the  $a_c$  and  $a_s$  propagators, respectively. The black and blue solid lines with arrows represent the  $\psi_{1,\pm,j}$  and  $\psi_{2,\pm,j}$  fermion propagators, respectively. All these twelve diagrams give a total contribution proportional to  $4 e_c^2 (\tilde{e}_c^2 + \tilde{e}_s^2)$ .

which again have a continuous line of fixed points defined by:

$$\frac{\tilde{e}_s^* + \tilde{e}_c^*}{N} = \frac{3\epsilon}{2u_0 + u_1} - \frac{18(2v_0 + v_1 - 3w)}{(2u_0 + u_1)^3} \epsilon^2 + \mathcal{O}(\epsilon^3). \quad (52)$$

However, at three-loop order, there are diagrams giving rise to terms in the beta functions which are not proportional to  $(\tilde{e}_s + \tilde{e}_c)$  raised to some integer power. Some of them are shown in Fig. 3, which are the Aslamazov-Larkin diagrams in the particle-particle channels contributing to the self-energy of the  $a_c$  transverse gauge field. All these twelve diagrams give a total contribution proportional to  $4 e_c^2 (\tilde{e}_c^2 + \tilde{e}_s^2)$ . Similarly, the Aslamazov-Larkin diagrams in the particle-hole channels will contribute with a term proportional to  $4 e_c^2 (\tilde{e}_c^2 + \tilde{e}_s^2)$ . One can also easily conclude that such corrections to the self-energy of the  $a_s$  transverse gauge field will be proportional to  $4 e_s^2 (\tilde{e}_c^2 + \tilde{e}_s^2)$ . Note that if the two fermions had carried the same charge under the two gauge fields, then the contributions would have been proportional to  $4 e_c^2 (\tilde{e}_c + \tilde{e}_s)^2$  and  $4 e_s^2 (\tilde{e}_c + \tilde{e}_s)^2$ , respectively, for the  $a_c$  and  $a_s$  fields, leading to the preservation of the fixed line feature.

For  $m > 1$ , the UV/IR mixing will render the higher-loop corrections to be  $k_F$ -suppressed and hence they will have no effect on the fixed line. Therefore, the fixed line feature is generically not altered by going to higher loops.

#### IV. Conclusion

In this paper, we have applied the dimensional regularization scheme, developed for non-Fermi liquids arising at Ising-nematic quantum critical point, to the case of non-Fermi liquids arising from transverse gauge field couplings with finite-density fermions. This has allowed us to access the interacting fixed points perturbatively in an expansion in  $\epsilon$ , which is the difference between the upper critical dimension ( $d_c = m + \frac{3}{m+1}$ ) and the actual physical dimension ( $d_{\text{phys}} = m + 1$ ) of the theory, for a Fermi surface of dimension  $m$ . We have extracted the scaling behaviour for the case of one and two  $U(1)$  gauge fields.

There is a crucial difference in the matrix structure of the couplings in the cases of Ising-nematic order parameter and gauge fields. This arises from the fact that the fermions on the antipodal points of the Fermi surface couple to the Ising-nematic order parameter (transverse gauge) with the same (opposite) sign(s). Hence, although we get the same values of critical dimension and critical exponents, the differences will show up in the renormalization of some physical quantities like the  $2k_F$  scattering (backscattering involving an operator that carries a momentum  $2k_F$ ) amplitudes.

The  $U(1) \times U(1)$  is particularly interesting in the context of recent works which show that this scenario is useful to describe the phenomena of deconfined Mott transition, and deconfined metal-metal transition [56]. In Ref. 56, Zou and Chowdhury found that in  $(2+1)$  spacetime dimensions and at one-loop order, these systems exhibited a continuous

line of stable fixed points, rather than a single one. Their method involved modifying the bosonic dispersion (such that it becomes nonanalytic in the momentum space), and then carrying out a double expansion in two small parameters [10, 17]. Our method avoids this issue by employing the dimensional regularization scheme. We also have the advantage that we could analyze a critical Fermi surface of generic dimensions, and also perform higher-loop diagrams giving order by order corrections in  $\epsilon$ . The discovery of a fixed line for the  $U(1) \times U(1)$  theory in Ref. [56] raised the question whether this feature survives when we consider either higher dimensions or higher loops. Our computations show that definitely higher dimensions do not reduce the fixed line to discrete fixed points. Regarding higher-loop corrections, we have not performed those explicitly, but through arguments based on the previous results for the Ising-nematic critical points [22, 24, 25], we have pre-

dicted that although the two-loop corrections will not make the fixed line degenerate into fixed point(s), the presence of certain three-loop diagrams will. In future, it will be worthwhile to carry out this entire procedure for the case of  $SU(2)$  gauge fields [56]. Another direction is to compute the RG flows for superconducting instabilities in presence of these transverse gauge fields, as was done in Ref. 27 for the Ising-nematic order parameter.

## Acknowledgments

We thank Debanjan Chowdhury for stimulating discussions. We are especially grateful to Andres Schlief for valuable comments on the manuscript. We also thank Sung-Sik Lee for pointing out that Aslamasov-Larkin diagrams will affect the fixed line feature at three-loop order.

- 
- [1] T. Holstein, R. E. Norton, and P. Pincus, “de haas-van alphen effect and the specific heat of an electron gas,” *Phys. Rev. B* **8**, 2649–2656 (1973).
- [2] M. Yu. Reizer, “Relativistic effects in the electron density of states, specific heat, and the electron spectrum of normal metals,” *Phys. Rev. B* **40**, 11571–11575 (1989).
- [3] Patrick A. Lee and Naoto Nagaosa, “Gauge theory of the normal state of high- $t_c$  superconductors,” *Phys. Rev. B* **46**, 5621–5639 (1992).
- [4] B. I. Halperin, Patrick A. Lee, and Nicholas Read, “Theory of the half-filled landau level,” *Phys. Rev. B* **47**, 7312–7343 (1993).
- [5] J. Polchinski, “Low-energy dynamics of the spinon-gauge system,” *Nuclear Physics B* **422**, 617–633 (1994).
- [6] B. L. Altshuler, L. B. Ioffe, and A. J. Millis, “Low-energy properties of fermions with singular interactions,” *Phys. Rev. B* **50**, 14048–14064 (1994).
- [7] S. Chakravarty, R. E. Norton, and O. F. Syljuåsen, “Transverse Gauge Interactions and the Vanquished Fermi Liquid,” *Physical Review Letters* **74**, 1423–1426 (1995).
- [8] E.-A. Kim, M. J. Lawler, P. Oreo, S. Sachdev, E. Fradkin, and S. A. Kivelson, “Theory of the nodal nematic quantum phase transition in superconductors,” *Phys. Rev. B* **77**, 184514 (2008).
- [9] C. Nayak and F. Wilczek, “Renormalization group approach to low temperature properties of a non-Fermi liquid metal,” *Nuclear Physics B* **430**, 534–562 (1994).
- [10] C. Nayak and F. Wilczek, “Non-Fermi liquid fixed point in 2 + 1 dimensions,” *Nuclear Physics B* **417**, 359–373 (1994).
- [11] M. J. Lawler, D. G. Barci, V. Fernández, E. Fradkin, and L. Oxman, “Nonperturbative behavior of the quantum phase transition to a nematic Fermi fluid,” *Phys. Rev. B* **73**, 085101 (2006).
- [12] Sung-Sik Lee, “Low-energy effective theory of fermi surface coupled with  $u(1)$  gauge field in 2 + 1 dimensions,” *Phys. Rev. B* **80**, 165102 (2009).
- [13] Max A. Metlitski and Subir Sachdev, “Quantum phase transitions of metals in two spatial dimensions. i. ising-nematic order,” *Phys. Rev. B* **82**, 075127 (2010).
- [14] Max A. Metlitski and Subir Sachdev, “Quantum phase transitions of metals in two spatial dimensions. ii. spin density wave order,” *Phys. Rev. B* **82**, 075128 (2010).
- [15] A. Abanov and A. Chubukov, “Anomalous Scaling at the Quantum Critical Point in Itinerant Antiferromagnets,” *Physical Review Letters* **93**, 255702 (2004).
- [16] A. Abanov and A. V. Chubukov, “Spin-Fermion Model near the Quantum Critical Point: One-Loop Renormalization Group Results,” *Physical Review Letters* **84**, 5608–5611 (2000).
- [17] David F. Mross, John McGreevy, Hong Liu, and T. Senthil, “Controlled expansion for certain non-fermi-liquid metals,” *Phys. Rev. B* **82**, 045121 (2010).
- [18] H.-C. Jiang, M. S. Block, R. V. Mishmash, J. R. Garrison, D. N. Sheng, O. I. Motrunich, and M. P. A. Fisher, “Non-Fermi-liquid d-wave metal phase of strongly interacting electrons,” *Nature (London)* **493**, 39–44 (2013).
- [19] Suk Bum Chung, Ipsita Mandal, Srinivas Raghu, and Sudip Chakravarty, “Higher angular momentum pairing from transverse gauge interactions,” *Phys. Rev. B* **88**, 045127 (2013).
- [20] Zhiqiang Wang, Ipsita Mandal, Suk Bum Chung, and Sudip Chakravarty, “Pairing in half-filled landau level,” *Annals of Physics* **351**, 727 – 738 (2014).
- [21] Shouvik Sur and Sung-Sik Lee, “Chiral non-fermi liquids,” *Phys. Rev. B* **90**, 045121 (2014).
- [22] Denis Dalidovich and Sung-Sik Lee, “Perturbative non-fermi liquids from dimensional regularization,” *Phys. Rev. B* **88**, 245106 (2013).
- [23] Shouvik Sur and Sung-Sik Lee, “Quasilocal strange metal,” *Phys. Rev. B* **91**, 125136 (2015).
- [24] Ipsita Mandal and Sung-Sik Lee, “Ultraviolet/infrared mixing in non-fermi liquids,” *Phys. Rev. B* **92**, 035141 (2015).
- [25] Ipsita Mandal, “UV/IR Mixing In Non-Fermi Liquids: Higher-Loop Corrections In Different Energy Ranges,” *Eur. Phys. J. B* **89**, 278 (2016).
- [26] Andreas Eberlein, Ipsita Mandal, and Subir Sachdev, “Hyperscaling violation at the ising-nematic quantum critical point in two-dimensional metals,” *Phys. Rev. B* **94**, 045133

- (2016).
- [27] Ipsita Mandal, “Superconducting instability in non-fermi liquids,” *Phys. Rev. B* **94**, 115138 (2016).
- [28] Ipsita Mandal, “Scaling behaviour and superconducting instability in anisotropic non-fermi liquids,” *Annals of Physics* **376**, 89 – 107 (2017).
- [29] Andres Schlierf, Peter Lunts, and Sung-Sik Lee, “Exact critical exponents for the antiferromagnetic quantum critical metal in two dimensions,” *Phys. Rev. X* **7**, 021010 (2017).
- [30] Peter Lunts, Andres Schlierf, and Sung-Sik Lee, “Emergence of a control parameter for the antiferromagnetic quantum critical metal,” *Phys. Rev. B* **95**, 245109 (2017).
- [31] Sung-Sik Lee, “Recent developments in non-fermi liquid theory,” *Annual Review of Condensed Matter Physics* **9**, 227244 (2018).
- [32] Dimitri Pimenov, Ipsita Mandal, Francesco Piazza, and Matthias Punk, “Non-fermi liquid at the fflo quantum critical point,” *Phys. Rev. B* **98**, 024510 (2018).
- [33] A. A. Abrikosov, “Calculation of critical indices for zero-gap semiconductors,” *JETP* **39**, 709–716 (1974).
- [34] Eun-Gook Moon, Cenke Xu, Yong Baek Kim, and Leon Balents, “Non-fermi-liquid and topological states with strong spin-orbit coupling,” *Phys. Rev. Lett.* **111**, 206401 (2013).
- [35] Rahul M. Nandkishore and S. A. Parameswaran, “Disorder-driven destruction of a non-fermi liquid semimetal studied by renormalization group analysis,” *Phys. Rev. B* **95**, 205106 (2017).
- [36] Ipsita Mandal and Rahul M. Nandkishore, “Interplay of Coulomb interactions and disorder in three-dimensional quadratic band crossings without time-reversal symmetry and with unequal masses for conduction and valence bands,” *Phys. Rev. B* **97**, 125121 (2018).
- [37] O. I. Motrunich, “Variational study of triangular lattice spin-1/2 model with ring exchanges and spin liquid state in  $\kappa$ - (ET)<sub>2</sub> Cu<sub>2</sub> (CN)<sub>3</sub>,” *Phys. Rev. B* **72**, 045105 (2005), [cond-mat/0412556](#).
- [38] Sung-Sik Lee and Patrick A. Lee, “U(1) gauge theory of the hubbard model: Spin liquid states and possible application to  $\kappa$ -(BEDT-TTF)<sub>2</sub>cu<sub>2</sub>(CN)<sub>3</sub>,” *Phys. Rev. Lett.* **95**, 036403 (2005).
- [39] P. A. Lee, N. Nagaosa, and X.-G. Wen, “Doping a Mott insulator: Physics of high-temperature superconductivity,” *Reviews of Modern Physics* **78**, 17–85 (2006).
- [40] Olexei I. Motrunich and Matthew P. A. Fisher, “ $d$ -wave correlated critical bose liquids in two dimensions,” *Phys. Rev. B* **75**, 235116 (2007).
- [41] Vadim Oganesyan, Steven A. Kivelson, and Eduardo Fradkin, “Quantum theory of a nematic fermi fluid,” *Phys. Rev. B* **64**, 195109 (2001).
- [42] W. Metzner, D. Rohe, and S. Andergassen, “Soft fermi surfaces and breakdown of fermi-liquid behavior,” *Phys. Rev. Lett.* **91**, 066402 (2003).
- [43] Luca Dell’Anna and Walter Metzner, “Fermi surface fluctuations and single electron excitations near pomeranchuk instability in two dimensions,” *Phys. Rev. B* **73**, 045127 (2006).
- [44] Hae-Young Kee, Eugene H. Kim, and Chung-Hou Chung, “Signatures of an electronic nematic phase at the isotropic-nematic phase transition,” *Phys. Rev. B* **68**, 245109 (2003).
- [45] Jérôme Rech, Catherine Pépin, and Andrey V. Chubukov, “Quantum critical behavior in itinerant electron systems: Eliashberg theory and instability of a ferromagnetic quantum critical point,” *Phys. Rev. B* **74**, 195126 (2006).
- [46] P. Wölfle and A. Rosch, “Fermi Liquid Near a Quantum Critical Point,” *Journal of Low Temperature Physics* **147**, 165–177 (2007).
- [47] Dmitrii L. Maslov and Andrey V. Chubukov, “Fermi liquid near pomeranchuk quantum criticality,” *Phys. Rev. B* **81**, 045110 (2010).
- [48] J. Quintanilla and A. J. Schofield, “Pomeranchuk and topological Fermi surface instabilities from central interactions,” *Phys. Rev. B* **74**, 115126 (2006), [cond-mat/0601103](#).
- [49] H. Yamase and H. Kohno, “Instability toward Formation of Quasi-One-Dimensional Fermi Surface in Two-Dimensional t-J Model,” *Journal of the Physical Society of Japan* **69**, 2151 (2000).
- [50] Hiroyuki Yamase, Vadim Oganesyan, and Walter Metzner, “Mean-field theory for symmetry-breaking fermi surface deformations on a square lattice,” *Phys. Rev. B* **72**, 035114 (2005).
- [51] Christoph J. Halboth and Walter Metzner, “ $d$ -wave superconductivity and pomeranchuk instability in the two-dimensional hubbard model,” *Phys. Rev. Lett.* **85**, 5162–5165 (2000).
- [52] P. Jakubczyk, P. Strack, A. A. Katanin, and W. Metzner, “Renormalization group for phases with broken discrete symmetry near quantum critical points,” *Phys. Rev. B* **77**, 195120 (2008).
- [53] Mario Zacharias, Peter Wölfle, and Markus Garst, “Multiscale quantum criticality: Pomeranchuk instability in isotropic metals,” *Phys. Rev. B* **80**, 165116 (2009).
- [54] Y. Huh and S. Sachdev, “Renormalization group theory of nematic ordering in  $d$ -wave superconductors,” *Phys. Rev. B* **78**, 064512 (2008).
- [55] T. Senthil and R. Shankar, “Fermi surfaces in general codimension and a new controlled nontrivial fixed point,” *Phys. Rev. Lett.* **102**, 046406 (2009).
- [56] Liujun Zou and Debanjan Chowdhury, “Deconfined metallic quantum criticality: a  $U(2)$  gauge theoretic approach,” arXiv e-prints (2020), [arXiv:2002.02972 \[cond-mat.str-el\]](#).
- [57] The  $k_F$ -dependence drops out for  $m = 1$ .
- [58] While performing the integral for  $k_{d-m+1}$ , we can neglect the contribution from the exponential term as  $k_{d-m+1}$  already appears in the denominator and is appropriately damped. For extracting leading order singular behaviour in  $k_F$ , this is sufficient.

## A. Computation Of The Feynman Diagrams At One-Loop Order

### 1. One-Loop Boson Self-Energy

In this subsection, we compute the one-loop boson self-energy:

$$\Pi_1(q) = -e^2 \mu^x \int dk \text{Tr} [\gamma_0 G_0(k+q) \gamma_0 G_0(k)] = 2e^2 \mu^x \int dk \frac{k_0(k_0+q_0) - \tilde{\mathbf{K}} \cdot (\tilde{\mathbf{K}} + \tilde{\mathbf{Q}}) - \delta_q \delta_{k+q}}{[\mathbf{K}^2 + \delta_k^2] [(\mathbf{K} + \mathbf{Q})^2 + \delta_{k+q}^2]} e^{-\frac{\mathbf{L}_{(k)}^2 + \mathbf{L}_{(k+q)}^2}{\mu \tilde{k}_F}}. \quad (\text{A1})$$

We first integrate over  $k_{d-m}$  to obtain [58]:

$$\begin{aligned} \Pi_1(q) &= e^2 \mu^x \int \frac{d\mathbf{L}_{(k)} d\mathbf{K}}{(2\pi)^d} \frac{2k_0(k_0+q_0) - \mathbf{K} \cdot (\mathbf{K} + \mathbf{Q})}{|\mathbf{K}| |\mathbf{K} + \mathbf{Q}| \left[ (\delta_q + 2\mathbf{L}_{(q)}^i \mathbf{L}_{(k)}^i)^2 + (|\mathbf{K} + \mathbf{Q}| + |\mathbf{K}|)^2 \right]} (|\mathbf{K} + \mathbf{Q}| + |\mathbf{K}|) e^{-\frac{\mathbf{L}_{(k)}^2 + \mathbf{L}_{(k+q)}^2}{\mu \tilde{k}_F}} \\ &\quad - e^2 \mu^x \int \frac{d\mathbf{L}_{(k)} d\mathbf{K}}{(2\pi)^d} \frac{|\mathbf{K} + \mathbf{Q}| + |\mathbf{K}|}{(\delta_q + 2\mathbf{L}_{(q)}^i \mathbf{L}_{(k)}^i)^2 + (|\mathbf{K} + \mathbf{Q}| + |\mathbf{K}|)^2} \times e^{-\frac{\mathbf{L}_{(k)}^2 + \mathbf{L}_{(k+q)}^2}{\mu \tilde{k}_F}}, \end{aligned} \quad (\text{A2})$$

where we have chosen the coordinate system such that  $\mathbf{L}_{(q)} = (q_{d-m+1}, 0, 0, \dots, 0)$ . Since the problem is rotationally invariant in these directions and  $\Pi_1(q)$  depends only on the magnitude of  $\mathbf{L}_{(q)}$ , the final result is independent of this choice.

Making a change of variable,  $u = \delta_q + 2q_{d-m+1}k_{d-m+1}$ , and integrating over  $u$ , we get

$$I \equiv \int \frac{dk_{d-m+1}}{2\pi} \frac{1}{(\delta_q + 2q_{d-m+1}k_{d-m+1})^2 + (|\mathbf{K} + \mathbf{Q}| + |\mathbf{K}|)^2} = \frac{1}{4|\mathbf{L}_{(q)}| (|\mathbf{K} + \mathbf{Q}| + |\mathbf{K}|)}. \quad (\text{A3})$$

The rest of  $\mathbf{L}_{(k)}$ -integrals evaluate to  $J^{m-1}$ , where

$$J \equiv \int_{-\infty}^{\infty} \frac{dy}{2\pi} \exp \left\{ \frac{-2y^2}{\mu \tilde{k}_F} \right\} = \sqrt{\frac{\mu \tilde{k}_F}{8\pi}}. \quad (\text{A4})$$

Hence the self-energy expression reduces to:

$$\Pi_1(q) = \frac{e^2 \mu^x}{2^{m+1} |\mathbf{L}_{(q)}|} \left( \frac{\mu \tilde{k}_F}{2\pi} \right)^{\frac{m-1}{2}} I_1(d-m, \mathbf{Q}), \quad (\text{A5})$$

where

$$I_1(d-m, \mathbf{Q}) = \int \frac{d\mathbf{K}}{(2\pi)^{d-m}} \left[ \frac{k_0(k_0+q_0) - \tilde{\mathbf{K}} \cdot (\tilde{\mathbf{K}} + \tilde{\mathbf{Q}})}{|\mathbf{K} + \mathbf{Q}| |\mathbf{K}|} - 1 \right]. \quad (\text{A6})$$

The  $(d-m)$ -dimensional integral in  $I_1(d-m, \mathbf{Q})$  can be done using the Feynman parametrization formula

$$\frac{1}{A^\alpha B^\beta} = \frac{\Gamma(\alpha + \beta)}{\Gamma(\alpha) \Gamma(\beta)} \int_0^1 dt \frac{t^{\alpha-1} (1-t)^{\beta-1}}{[tA + (1-t)B]^{\alpha+\beta}}. \quad (\text{A7})$$

Substituting  $\alpha = \beta = 1/2$ ,  $A = |\mathbf{K} + \mathbf{Q}|^2$  and  $B = |\mathbf{K}|^2$ , we get:

$$I_1(d-m, \mathbf{Q}) = \frac{1}{\pi (2\pi)^{d-m}} \int_0^1 \frac{dt}{\sqrt{t(1-t)}} \int d\mathbf{K} \left[ \frac{k_0(k_0+q_0) - \tilde{\mathbf{K}} \cdot (\tilde{\mathbf{K}} + \tilde{\mathbf{Q}})}{x |\mathbf{K} + \mathbf{Q}|^2 + (1-t)\mathbf{K}^2} - 1 \right]. \quad (\text{A8})$$

Introducing the new variable  $\mathbf{u} = \mathbf{K} + t\mathbf{Q}$ ,  $I_1$  reduces to:

$$I_1(d-m, \mathbf{Q}) = \frac{1}{\pi (2\pi)^{d-m}} \int_0^1 \frac{dt}{\sqrt{t(1-t)}} \int d^{d-m} \mathbf{u} \left[ \frac{2 \{ u_0^2 - t(1-t)q_0^2 \} - 2\mathbf{u}^2}{\mathbf{u}^2 + t(1-t)\mathbf{Q}^2} \right]. \quad (\text{A9})$$

Again, we use another new variable  $\mathbf{v}$ , defined by  $\mathbf{u} = \sqrt{t(1-t)} \mathbf{v}$ , so that

$$I_1(d-m, \mathbf{Q}) = -\frac{2^{-2d+2m+1} \pi^{-d+m+\frac{1}{2}} \Gamma\left(\frac{d-m+1}{2}\right)}{\Gamma\left(\frac{d-m+2}{2}\right)} \int d^{d-m} \mathbf{v} \frac{q_0^2 + \tilde{\mathbf{v}}^2}{\mathbf{v}^2 + \mathbf{Q}^2}. \quad (\text{A10})$$

Using

$$\int_0^\infty dy \frac{y^{n_1}}{(y^2 + C)^{n_2}} = \frac{\Gamma\left(\frac{n_1+1}{2}\right) \Gamma\left(n_2 - \frac{n_1+1}{2}\right)}{2 \Gamma(n_2)} C^{\frac{n_1+1}{2} - n_2}, \quad (\text{A11})$$

and the volume of the  $(n-1)$ -sphere (at the boundary of the  $n$ -ball of unit radius)

$$S^{n-1} \equiv \int d\Omega_n = \frac{2\pi^{n/2}}{\Gamma(n/2)}, \quad (\text{A12})$$

we finally obtain the one-loop boson self-energy to be:

$$\Pi_1(k) = -\frac{\beta(d, m) e^2 \mu^x}{|\mathbf{L}_{(q)}|} \left(\mu \tilde{k}_F\right)^{\frac{m-1}{2}} \left[k_0^2 + (m+1-d) \tilde{\mathbf{K}}^2\right] |\mathbf{K}|^{d-m-2}, \quad (\text{A13})$$

with

$$\beta(d, m) = \frac{1}{2^{m+1}} \left(\frac{1}{2\pi}\right)^{\frac{m-1}{2}} \frac{2^{-2d+2m+1} \pi^{\frac{-d+m+3}{2}} \Gamma(d-m) \Gamma(m+1-d)}{\Gamma^2\left(\frac{d-m+2}{2}\right) \Gamma\left(\frac{m+1-d}{2}\right)} = \frac{2^{\frac{1+m-4d}{2}} \pi^{\frac{4-d}{2}} \Gamma(d-m) \Gamma(m+1-d)}{\Gamma^2\left(\frac{d-m+2}{2}\right) \Gamma\left(\frac{m+1-d}{2}\right)}. \quad (\text{A14})$$

## 2. One-Loop Fermion Self-Energy

Here we compute the one-loop fermion self-energy  $\Sigma_1(q)$  by using the dressed propagator for boson which includes the one-loop self-energy  $\Pi_1(k)$ :

$$\Sigma_1(q) = \frac{e^2 \mu^x}{N} \int dk \gamma_0 G_0(k+q) \gamma_0 D_1(k) = \frac{i e^2 \mu^x}{N} \int dk D_1(k) \frac{\tilde{\Gamma} \cdot (\tilde{\mathbf{K}} + \tilde{\mathbf{Q}}) + \gamma_{d-m} \delta_{k+q} - \gamma_0 (k_0 + q_0)}{(\mathbf{K} + \mathbf{Q})^2 + \delta_{k+q}^2} e^{-\frac{\mathbf{L}_{(k+q)}^2}{\mu \tilde{k}_F}}. \quad (\text{A15})$$

Integrating over  $k_{d-m}$ , we get

$$\Sigma_1(q) = \frac{i e^2 \mu^x}{2N} \int \frac{d^d k}{(2\pi)^d} D_1(k) \frac{\tilde{\Gamma} \cdot (\tilde{\mathbf{K}} + \tilde{\mathbf{Q}}) - \gamma_0 (k_0 + q_0)}{|\mathbf{K} + \mathbf{Q}|} \times e^{-\frac{\mathbf{L}_{(k+q)}^2}{\mu \tilde{k}_F}}. \quad (\text{A16})$$

Since only  $D_1(k) e^{-\frac{\mathbf{L}_{(k+q)}^2}{\mu \tilde{k}_F}}$  depends on  $\mathbf{L}_{(k)}$ , let us first perform the integral:

$$I_2(k) \equiv \int \frac{d\mathbf{L}_{(k)}}{(2\pi)^m} \frac{e^{-\frac{\mathbf{L}_{(q+k)}^2}{\mu \tilde{k}_F}}}{\mathbf{L}_{(k)}^2 + \beta_{dm} e^2 \mu^x (\mu \tilde{k}_F)^{\frac{m-1}{2}} \frac{|\mathbf{K}|^{d-m}}{|\mathbf{L}_{(k)}|} \times \left[d - m - 1 + (m-d) \frac{k_0^2}{|\mathbf{K}|^2}\right]} \\ = \frac{\pi^{\frac{2-m}{2}}}{3 \times 2^{m-1} \Gamma(m/2) |\sin\{(m+1)\pi/3\}| \left[\beta(d, m) e^2 \mu^x (\mu \tilde{k}_F)^{\frac{m-1}{2}} |\mathbf{K}|^{d-m-2} \times \left\{k_0^2 + (m+1-d) \tilde{\mathbf{K}}^2\right\}\right]^{\frac{2-m}{3}}}. \quad (\text{A17})$$

Now the expression for the self-energy can be written as:

$$\Sigma_1(q) = \frac{i e^{2(m+1)/3} \mu^x (m+1)/3 \pi^{\frac{2-m}{2}} \times I_3(d-m, \mathbf{Q})}{6N \times 2^{m-1} \Gamma(m/2) |\sin(\frac{m+1}{3}\pi)| [\beta(d, m)]^{\frac{2-m}{3}} (\mu \tilde{k}_F)^{(m-1)(2-m)/6}}, \quad (\text{A18})$$

where

$$\begin{aligned}
I_3(d-m, \mathbf{Q}) &= \int \frac{d\mathbf{K}}{(2\pi)^{d-m}} \frac{\tilde{\Gamma} \cdot (\tilde{\mathbf{K}} + \tilde{\mathbf{Q}}) - \gamma_0 (k_0 + q_0)}{\left[ \left\{ k_0^2 + (m+1-d) \tilde{\mathbf{K}}^2 \right\} |\mathbf{K}|^{d-m-2} \right]^{\frac{2-m}{3}} |\mathbf{K} + \mathbf{Q}|} \\
&= \frac{\Gamma\left(\frac{2d+m^2+3-m(d+2)}{6}\right)}{\Gamma\left(\frac{1}{2}\right) \Gamma\left(\frac{2-m}{3}\right) \Gamma\left(\frac{(d-m-2)(2-m)}{6}\right)} \int_0^1 dt_1 \int_0^{1-t_1} dt_2 \frac{(1-t_1-t_2)^{\frac{(d-m-2)(2-m)}{6}-1}}{t_1^{\frac{m+1}{3}} \sqrt{t_2}} \\
&\quad \times \int \frac{d\mathbf{K}}{(2\pi)^{d-m}} \frac{\tilde{\Gamma} \cdot (\tilde{\mathbf{K}} + \tilde{\mathbf{Q}}) - \gamma_0 (1-t_2) q_0}{\left[ t_1 (m+1-d) \tilde{\mathbf{K}}^2 + t_2 (\tilde{\mathbf{K}} + \tilde{\mathbf{Q}})^2 + (1-t_1-t_2) \tilde{\mathbf{K}}^2 + q_0^2 t_2 (1-t_2) + k_0^2 \right]^{\frac{2d+m^2+3-m(d+2)}{6}}} \\
&= \frac{\pi^{\frac{m-d-1}{2}} \Gamma\left(\frac{3-(d-m)(m+1)}{6}\right)}{2^{d-m} \Gamma\left(\frac{2-m}{3}\right) \Gamma\left(\frac{m^2-d(m-2)-4}{6}\right)} \int_0^1 dt_1 \int_0^{1-t_1} dt_2 \left[ \frac{(1-t_1-t_2)^{\frac{(d-m-2)(2-m)}{6}-1}}{t_1^{\frac{m+1}{3}} \sqrt{t_2}} \frac{\gamma_0 (1-t_2) q_0 - (\tilde{\Gamma} \cdot \tilde{\mathbf{Q}}) \left[ \frac{(1+m t_1 - d t_1 - t_2)}{1+m t_1 - d t_1} \right]}{(1+m t_1 - d t_1)^{\frac{(d-m)(2-m)}{6}}} \right. \\
&\quad \left. \left\{ \frac{\tilde{\mathbf{Q}}^2 t_2 (1+m t_1 - d t_1 - t_2)}{(1+m t_1 - d t_1)^2} + \frac{q_0^2 t_2 (1-t_2)}{1+m t_1 - d t_1} \right\}^{\frac{(d-m)(m+1)-3}{6}} \{ \Theta(1+m t_1 - d t_1) + fac \times \Theta(d t_1 - 1 - m t_1) \} \right]. \tag{A19}
\end{aligned}$$

where  $fac = (-1)^{\frac{(m-2)(d-m)}{3}} i^{d-m+1} \left[ (-1)^{\frac{1}{6}(m-2)(m-d)} \cos\left(\frac{(m+1)(d-m)}{6}\pi\right) - \cos\left(\frac{d-m}{2}\pi\right) \right] \csc\left(\frac{(m-2)(d-m)}{6}\pi\right)$ . From this expression, it is clear that  $I_3(d-m, \mathbf{Q})$  blows up when the argument of the gamma function in the numerator blows up, i.e.  $\frac{3-(d-m)(m+1)}{6} = 0$ . This implies that  $\Sigma_1(q)$  blows up logarithmically in  $\Lambda$  at the critical dimension

$$d_c(m) = m + \frac{3}{m+1}. \tag{A20}$$

The integrals over  $t_1$  and  $t_2$  are convergent, but their values have to be computed numerically for a given  $m$ .

Expanding in  $\epsilon$  defined as  $d = m + \frac{3}{m+1} - \epsilon$ , we obtain:

$$\Sigma_1(q) = -\frac{i e^{\frac{2(m+1)}{3}} \left[ u_0 \left( \frac{\mu}{|q_0|} \right)^{\frac{m+1}{3}\epsilon} \gamma_0 q_0 + u_1 \left( \frac{\mu}{|\mathbf{Q}|} \right)^{\frac{m+1}{3}\epsilon} (\tilde{\Gamma} \cdot \tilde{\mathbf{Q}}) \right]}{N \tilde{k}_F^{\frac{(m-1)(2-m)}{6}} \epsilon} + \text{finite terms}, \tag{A21}$$

where  $u_0, u_1 \geq 0$ . Numerically, we find:

$$\begin{cases} u_0 = 0.0201044, & v_0 = 1.85988 \quad \text{for } m = 1 \\ u_0 = v_0 = 0.0229392 & \quad \text{for } m = 2 \end{cases}. \tag{A22}$$

### 3. One-Loop Vertex Correction

In general, the one-loop fermion-boson vertex function  $\Gamma_1(k, q)$  depends on both  $k$  and  $q$ . In order to extract the leading  $1/\epsilon$  divergence, however, it is enough to look at the  $q \rightarrow 0$  limit. In this limit, we get

$$\begin{aligned} \Gamma_1(k, 0) &= \frac{e^2 \mu^x}{N} \int \frac{d^{d+1}q}{(2\pi)^{d+1}} \gamma_0 G_0(q) \gamma_0 G_0(q) \gamma_0 D_1(q - k) \\ &= \frac{e^2 \mu^x}{N} \int \frac{d^{d+1}q}{(2\pi)^{d+1}} D_1(q - k) \gamma_0 \left[ \frac{1}{\mathbf{Q}^2 + q_{d-m}^2} - \frac{2q_0^2}{(q_0^2 + \tilde{\mathbf{Q}}^2 + q_{d-m}^2)^2} \right] e^{-\frac{2\mathbf{L}_q^2}{\mu k_F}} \\ &= \frac{e^2 \mu^x}{2N} \int \frac{d\mathbf{Q} d\mathbf{L}_q}{(2\pi)^d} D_1(q) \gamma_0 \frac{(\tilde{\mathbf{Q}} + \tilde{\mathbf{K}})^2}{[(q_0 + k_0^2)^2 + (\tilde{\mathbf{Q}} + \tilde{\mathbf{K}})^2]^{3/2}} e^{-\frac{2\mathbf{L}_q^2}{\mu k_F}}. \end{aligned} \quad (\text{A23})$$

Using Eq. (A17), the above expression reduces to

$$\Gamma_1(k, 0) = \frac{e^2 \mu^x \gamma_0}{N} \frac{\pi^{\frac{m}{2}+1-d}}{3 \times 2^d \Gamma(m/2) |\sin(\frac{m+1}{3}\pi)| \left[ \beta(d, m) e^2 \mu^x (\mu k_F)^{\frac{m-1}{2}} \right]^{\frac{2-m}{3}}} \times I_4(d, m), \quad (\text{A24})$$

where

$$\begin{aligned} I_4(d, m) &= \int \frac{d\mathbf{Q}}{\left[ |\mathbf{Q}|^{d-m-2} \left\{ q_0^2 + (m+1-d)\tilde{\mathbf{Q}}^2 \right\} \right]^{\frac{2-m}{3}}} \frac{(\tilde{\mathbf{Q}} + \tilde{\mathbf{K}})^2}{\left[ (q_0 + k_0^2)^2 + (\tilde{\mathbf{Q}} + \tilde{\mathbf{K}})^2 \right]^{3/2}} \\ &= \int_0^1 dt_1 \int_0^{1-t_1} dt_2 \frac{\Gamma\left(\frac{2d+m^2+9-m(d+2)}{6}\right) t_1^{-\frac{m+1}{3}} t_2^{\frac{1}{2}} (1-t_1-t_2)^{\frac{(d-m-2)(2-m)}{6}-1}}{\Gamma\left(\frac{3}{2}\right) \Gamma\left(\frac{2-m}{3}\right) \Gamma\left(\frac{(d-m-2)(2-m)}{6}\right)} \\ &\quad \times \int \frac{d\mathbf{Q}}{(2\pi)^{d-m}} \frac{(\tilde{\mathbf{Q}} + \tilde{\mathbf{K}})^2}{\left[ t_1(m+1-d)\tilde{\mathbf{Q}}^2 + t_2(\tilde{\mathbf{Q}} + \tilde{\mathbf{K}})^2 + (1-t_1-t_2)\tilde{\mathbf{Q}}^2 + k_0^2 t_2(1-t_2) + q_0^2 \right]^{\frac{-(d+2)m+2d+m^2+9}{6}}} \\ &= \int_0^1 dt_1 \int_0^{1-t_1} dt_2 \frac{\Gamma\left(\frac{2d+m^2+9-m(d+2)}{6}\right) t_1^{-\frac{m+1}{3}} t_2^{\frac{1}{2}} (1-t_1-t_2)^{\frac{(d-m-2)(2-m)}{6}-1}}{\Gamma\left(\frac{3}{2}\right) \Gamma\left(\frac{2-m}{3}\right) \Gamma\left(\frac{(d-m-2)(2-m)}{6}\right)} \times \frac{\Gamma\left(\frac{(d-m)(2-m)}{6} + 1\right)}{\Gamma\left(\frac{m^2-(d+2)m+2d+9}{6}\right)} \\ &\quad \times \frac{J_1}{(1+m t_1 - d t_1)^{\frac{(d-m)(m-2)-6}{6}}}. \end{aligned} \quad (\text{A25})$$

Here,

$$\begin{aligned} J_1 &= \int \frac{d\tilde{\mathbf{Q}}}{(2\pi)^{d-m}} \frac{\tilde{\mathbf{Q}}^2 + A^2}{\left[ \tilde{\mathbf{Q}}^2 + B \right]^{\frac{(d-m)(m-2)-6}{6}}} \\ &= \frac{B^{\frac{5d+m^2+3-(d+5)m}{6}} \Gamma\left(\frac{(d-m)(m-5)-9}{6}\right)}{3 \times 2^{d-m+1} \pi^{\frac{d-m+1}{2}} \Gamma\left(\frac{(d-m)(m-2)}{6} - 1\right)} \left[ \{(d-m)(m-5) - 9\} A^2 + 3(d-m-1)B \right], \end{aligned} \quad (\text{A26})$$

where  $B \equiv \frac{\tilde{\mathbf{K}}^2 t_2 (1+m t_1 - d t_1 - t_2)}{(1+m t_1 - d t_1)^2} + \frac{k_0^2 t_2 (1-t_2)}{1+m t_1 - d t_1}$  and  $A^2 = \left( \frac{1+m t_1 - d t_1 - t_2}{1+m t_1 - d t_1} \right)^2 \tilde{\mathbf{K}}^2$ .

As demonstrated below, we find that although the final value has to be calculated numerically, the expression for  $\Gamma_1(k, 0)$  does not have any pole in  $\epsilon = m + \frac{3}{m+1} - \epsilon$  and is therefore non-divergent.

$$\Gamma_1(k, 0) = \begin{cases} -\frac{e^{2/3} \mu^{2\epsilon/3} \gamma_0}{N [\beta(\frac{5}{2}, 1)]^{1/3}} \times \frac{\Gamma(\frac{5}{4})}{180 \sqrt{3} \pi^{9/4} \Gamma(-\frac{5}{4}) \Gamma(-\frac{1}{12}) \Gamma(\frac{1}{3})^2} \int_0^1 dt_1 \int_0^{1-t_1} dt_2 \frac{t_2^{1/2} B^{3/2} (B-10A^2)}{t_1^{2/3} (1-t_1-t_2)^{13/12}} & \text{for } m = 1 \\ 0 & \text{for } m = 2 \end{cases} \quad (\text{A27})$$


---